GEOPHYSICAL RESEARCH LETTERS, VOL. 35, L04810, doi: 10.1029/2007GL032314, 2008

Click Here for Full Article

First observational estimates of global clear sky shortwave aerosol direct radiative effect over land

Falguni Patadia,[1] Pawan Gupta,[1] and Sundar A. Christopher[1]

Received 19 October 2007; revised 30 November 2007; accepted 17 January 2008; published 22 February 2008.

[1] Using one year (2000–2001) of merged Multiangle Imaging SpectroRadiometer (MISR), Moderate Resolution Imaging SpectroRadiometer (MODIS) and Clouds and the Earth's Radiant Energy System (CERES) data sets from NASA's Terra satellite, we estimate the top of atmosphere cloud-free direct radiative effect (DRE) of aerosols over global land areas. The global mean shortwave DRE is -5.1 ± 1.1 Wm^{-2} although substantial regional variability in DRE over land exists due to differences in aerosol properties and land cover types. This value is consistent with those reported in the literature although this is the first observational estimate of the global DRE over land using satellite data alone. Future studies need to separate the anthropogenic component of aerosols from satellite data to examine aerosol climate forcing over global scales.
Citation: Patadia, F., P. Gupta, and S. A. Christopher (2008), First observational estimates of global clear sky shortwave aerosol direct radiative effect over land, *Geophys. Res. Lett.*, *35*, L04810, doi:10.1029/2007GL032314.

1. Introduction

[2] Aerosols are key components of the climate system. The scattering properties of aerosols act to reduce solar insolation reaching the surface, increasing the amount of radiation scattered back to space thereby cooling the earth-atmosphere system while some aerosols such as black carbon also absorb solar radiation that can warm portions of the atmosphere [*Kaufman et al.*, 2002]. The difference between the reflected solar energy at the top of atmosphere without and with the presence of aerosols is called the direct radiative effect (DRE). This is the combined effect of all aerosols including those from both anthropogenic and natural sources [e.g., *Christopher and Zhang*, 2004]. The direct radiative effect from only anthropogenic aerosols is known as direct climate forcing (DCF) and necessitates the separation of natural from the anthropogenic aerosols, which is not the focus of this study.

[3] Recently, there has been an increasing emphasis towards assessing aerosol radiative impacts from observational methods [*Anderson et al.*, 2005]. Observational approaches either use satellite-retrieved aerosol optical thickness (AOT) coupled with radiative transfer calculations [e.g., *Bellouin et al.*, 2005] or use the same AOT values with coincident broadband radiative flux values that does not require radiative transfer calculations [e.g., *Christopher and Zhang*, 2004]. However, most satellite-based studies of aerosols have examined total aerosol effects rather than the anthropogenic components although new techniques are available to study DCF from space [*Kaufman et al.*, 2005]. These studies were largely confined to cloud-free oceans due to the difficulties in obtaining reliable aerosol information over land from multi-spectral data alone. Nevertheless, global estimates of aerosol effects have been achieved using a combination of models and observations [e.g., *Bellouin et al.*, 2005]. The TOA DRE for cloud-free oceans among a dozen measurement based studies is -5.5 Wm^{-2} with a standard error from the various methods of ± 0.2 Wm^{-2} [*Yu et al.*, 2006]. Considering the different techniques and data sets that were used there is a remarkable agreement among methods, although regional differences can be substantially larger [*Anderson et al.*, 2005]. One of the major reasons for this success is the availability of high quality satellite measurements of aerosols from the Moderate Resolution Imaging SpectroRadiometer (MODIS) [*Remer et al.*, 2005] and the Multi-angle Imaging SpectroRadiometer (MISR) [*Kahn et al.*, 2005]. For example, the Multiangle Imaging SpectroRadiometer (MISR) retrieves reliable AOT globally with an overall accuracy better than ± 0.05 or 20% [*Kahn et al.*, 2005] while the MODIS with 36 spectral channels provides superior cloud and aerosol identification capabilities and near daily aerosol retrievals over oceans that have been used in numerous studies for studying aerosol effects over oceans [*Yu et al.*, 2006].

[4] In this paper, we provide the first steps for estimating DRE over land using one year [2001] of merged MODIS, MISR and CERES datasets. The MODIS is used for cloud screening since it uses comprehensive high resolution multi-spectral information for cloud identification, the CERES is used to obtain TOA broadband shortwave fluxes, and the MISR is used to obtain AOT values within the CERES footprint. By using merged CERES fluxes and MISR AOT, we eliminate the need for radiative transfer calculations for obtaining the radiative fluxes needed to estimate the DRE of aerosols. This approach is similar to the one used by *Christopher and Zhang* [2004] although their study was limited to ocean regions. There are two reasons for using the MISR aerosol data product: (1) aerosol retrievals are available over all surfaces including bright targets such as deserts and other highly reflective urban areas and, (2) MISR retrievals compare better with AERONET when compared to MODIS AOT comparison with AERONET especially over high reflective targets and coastal sites where surface brightness and sub-pixel water contamination pose major problems [*Abdou et al.*, 2005]. However, one of the major disadvantages of the MISR is the narrow swath width of the sensor allowing global coverage only once in about 9 days

[1]Department of Atmospheric Sciences, University of Alabama in Huntsville, Huntsville, Alabama, USA.

Copyright 2008 by the American Geophysical Union.
0094-8276/08/2007GL032314$05.00

requiring multiple months of data to obtain a global view of aerosols and their radiative effects.

2. Data and Methodology

[5] We use data from CERES, MODIS, and MISR sensors onboard the Terra satellite. The TOA CERES radiances in the shortwave (0.3–5 μm), window (8–12 μm) and total channel (0.3–200 μm) are converted to TOA fluxes using angular distribution models [*Loeb et al.*, 2005] and are reported at 20 km spatial resolution (at nadir). Compared to previous generation of broadband sensors, the CERES derived fluxes have higher accuracy for clear and cloudy conditions, improving monthly mean TOA fluxes by nearly 1.8 Wm^{-2} in the shortwave and 1.3 Wm^{-2} in the longwave and these CERES fluxes have been successfully used by several studies to estimate DRE over ocean [e.g., *Zhang et al.*, 2005; *Loeb and Manalo-Smith*, 2005]. It should be noted that the current ADMs used to derive TOA fluxes over land from CERES measurements do not include the effect of aerosols.

[6] MISR onboard Terra observes TOA radiances in four channels (0.446 μm, 0.558 μm, 0.672 μm and 0.866 μm) at nine viewing angles (0°, ±26.1°, ±45.6°, ±60°, ±70.5°) over a 360 km swath [*Diner et al.*, 1998]. It has a global coverage of 9 days at the equator and 2 days at the poles. Using MISR observations, the aerosol properties are retrieved using pre-calculated look-up tables over a 17.6 km^2 region that contains 16 X 16 MISR pixels each with a 1.1 km^2 resolution. A detailed description of MISR aerosol retrieval is given by *Martonchik et al*. [1998, 2002]. In this study, we use one year (December 2000–November 2001) of CERES single scanner footprint (SSF) data that contains the merged CERES and MODIS data and we merge this with the level 2 MISR aerosol product (MIL2ASAE, version F09_0017) over global land areas [*Gupta et al.*, 2008]. *Loeb et al.* [2007] discuss the validation of the CERES fluxes and *Kahn et al.* [2005] discuss the strengths and limitations of the aerosol optical thickness product from MISR.

[7] Since the estimation of DRE requires coincident AOT and shortwave flux, we combine the MISR AOT with the CERES SSF data by collocating MISR observations within CERES footprint in space and time [*Gupta et al.*, 2008]. To avoid large pixel sizes, collocation is restricted to solar and viewing zenith angles less than 60°. DRE is defined as the difference between outgoing shortwave flux in clear (cloud and aerosol-free) and aerosol sky conditions [*Zhang et al.*, 2005] and is estimated at the CERES pixel resolution (20 km at nadir). CERES SSF product contains information on percentage cloud cover at every CERES pixel which is based on the MODIS cloud screening algorithm. We use the cloud cover information from the SSF product to cloud clear the merged MISR-CERES data. All pixels that are identified as 99.5% clear using MODIS data are used. The clear sky fluxes over land are obtained for *each season* using the regression relationship between cloud free MISR AOT and CERES SW flux in 0.5° × 0.5° latitude-longitude regions. The clear sky flux is the y-intercept of the regression line and corresponds to the TOA shortwave flux when AOT equals zero [*Zhang et al.*, 2005]. While it may be ideal to obtain clear sky fluxes at shorter space and time scales, the narrow swath width of the MISR and the stringent cloud-screening does not provide enough pixels at these scales. Cloud free pixels with valid MISR AOT values are then used to obtain aerosol sky fluxes. The difference between clear and aerosol shortwave fluxes at the satellite overpass time (~10:30 local time) is defined here as the instantaneous DRE. We convert the instantaneous DRE values to diurnal averages using methods outlined by *Remer and Kaufman* [2005]. We also correct for sample bias in DRE due to stringent cloud clearing and coarser resolution of the CERES instrument using methods outlined by *Zhang et al.* [2005]. Since the spatial resolution of MISR (17.6 km^2) is similar to that of CERES near nadir (20 km^2), the bias adjustment due to the coarse resolution of the CERES instrument is not significant, resulting in a lower overall bias adjustment compared to that used by *Zhang et al.* [2005]. The uncertainties associated with DRE estimation are discussed in section 3.

3. Results and Discussions

[8] Figure 1 shows the yearly mean spatial distribution of MISR AOT (λ = 0.558μm) within the CERES footprint (Figure 1a) and the DRE (Figure 1b) estimated from the merged data sets. Global desert regions were excluded from the analysis due to noisy relationships between MISR AOT and CERES shortwave fluxes which is to be expected due to the high surface albedo in these regions [*Hsu et al.*, 2000]. The global patterns of AOT compares well with the DRE patterns with large AOT and DRE values over Africa and South America primarily due to biomass burning [*Kaufman et al.*, 2002], and over India and China due to a combination of dust, smoke and pollution aerosols [*Kaufman et al.*, 2002]. Anthropogenic pollution over major cities also results in higher DRE values. Data over most parts of Indonesia is missing due to persistent cloud cover. However, a strong biomass burning signal can be seen in regions adjacent to Malaysia. Though Australia, Spain and central United States generally have low aerosol concentrations (AOT < 0.15), the DRE patterns match the AOT spatial distribution well, and remain largely negative. In contrast, large optical thicknesses in the Congo Basin, Ganges Valley and in eastern China do not translate to strong DRE values. These differences are due to the combined effects of aerosol and surface properties from diverse ecosystems. As aerosols become more absorbing, a critical threshold is reached, depending on their size and underlying surface, where the overall DRE can change from a negative to a positive effect. However, Figure 1 depicts *annual averages* over 1X1 degree grids where the positive and negative effects may average out and the annual-averaged net DRE is negative.

[9] The global mean DRE over land areas is −5.1 ± 1.1 Wm^{-2} corresponding to a mean MISR AOT (λ = 0.558μm) within the CERES footprint of 0.18. DRE in the Northern hemisphere (−5.2 Wm^{-2}) is 10% greater than in the Southern hemisphere (−4.75 Wm^{-2}). However, DRE varies significantly as a function of regions from −3.5 Wm^{-2} near Indonesia to −7.8 Wm^{-2} surrounding the Sahara desert (Figure 2). In comparison, *Yu et al.* [2006] use MISR AOT along with assumed aerosol properties in radiative transfer simulations and report DRE values of −5.45 and −4.75 Wm^{-2} for Northern and Southern hemi-

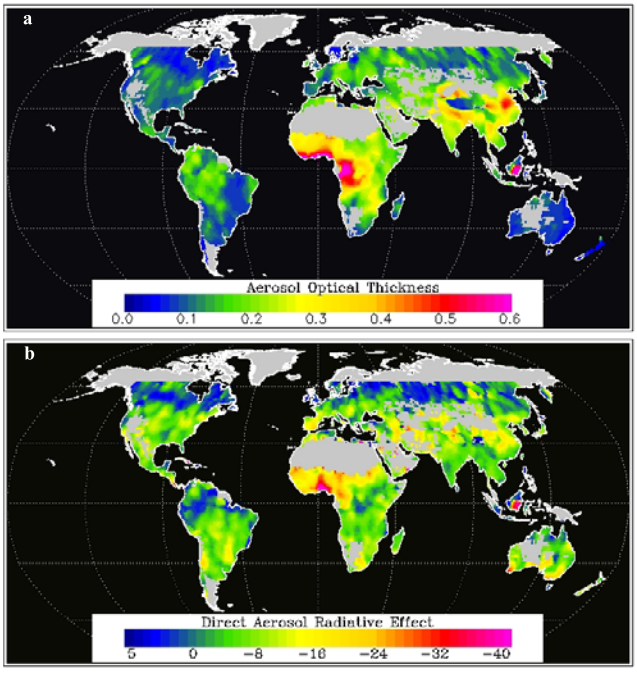

Figure 1. Spatial distribution of (a) annual mean MISR AOT (λ = 0.558μm), and (b) the TOA shortwave aerosol direct radiative effect (DRE) in Wm^{-2} for cloud-free conditions during year 2000–2001. Gray color on both AOT and DRE maps represents areas where analysis is not performed due to high solar zenith angles, lack of data, and inconsistent AOT-shortwave flux relations in regions with high surface reflectivity.

spheric regions respectively. There is a very good agreement between these two methods although our DRE estimate is larger by 0.2 Wm^{-2} that is within the estimated uncertainties.

[10] To further examine the regional patterns of AOT and DRE, we selected thirteen regions over the globe (Figure 2) that are same as that from *Yu et al.* [2006]. Regions 1–4 are from 30–60°N with longitude bins between 90°W–180°W, 0–90°W, 0–90°E, and 90°E–180°E, regions 5–8 use the same longitude bins but are for latitudes 0–30°N and regions 9–12 use the same longitude values but are for latitudes 0–30°S. Region 13 encompasses all longitudes between 30–60°S. The region bounded by 0–30°S and 90°W–180°W has very limited land area; thus, sample size is not large enough to produce meaningful statistics.

[11] Figure 2 shows the probability distribution functions of MISR AOT and diurnally averaged DRE for the 13 regions. The AOT and DRE show similar frequency distributions over land with some variations from one region to another. Regions 1, 2, 10 and 12 show a narrow distribution of low AOTs with broad distribution of DRE. In contrast, both AOT and DRE in regions 3, 6, 7, 8, and 11 show a broader distribution and higher AOTs. This corroborates well with Figure 1 where a broad distribution of AOT can result from the presence of different types of aerosols such as dust, smoke and pollution over India and China. In Figure 2, DRE shows a broader (narrower) distribution with less (more) contrast in the regions with wider (narrower) AOT distributions. Therefore, in Figure 1, we find that low AOT over Spain and Australia translate to a strong DRE while higher AOT in China and Congo basin do not. As noted earlier, different types of aerosol will have different size distributions and radiative properties that govern the AOT. On the other hand, DRE is a function of both the aerosol concentration, properties and the underlying surface reflectance. Therefore the net DRE is from the combined effect of the surface and aerosol properties.

[12] Figure 2 also shows a comparison between the mean AOT and DRE values for each region from satellite-model integrated estimates [*Yu et al.*, 2006] and from the present study. The difference in AOT varies from minimum of 0.01 in regions 6, 11, and 13 to maximum of 0.07 in regions 7, 8, and 12 with global mean difference of 0.05. DRE from these two studies also varies as a function of the regions. The difference varies from 0 to 1 Wm^{-2} in different regions except for zone 8 where the difference is as high as 3.7 Wm^{-2}. This difference could be associated with heterogeneous nature of aerosols (dust, pollution and smoke aerosols dominates in this part of the world during different season of the year) and the reduced number of samples. Overall differences are likely due to the use of different data sets and cloud screening techniques. *Yu et al.* [2006] used MISR level 3 1 × 1 degree MISR AOT values while we use the level 2 MISR AOT product at a higher spatial resolution of 17.6 × 17.6 km^2. Also, we use stringent cloud screening criteria to ensure that the CERES data are not contaminated with clouds while requiring 99.9% of the CERES footprint to be cloud free.

[13] While DRE estimation using multi-sensor observations may be more straightforward than performing model calculations, the uncertainties associated with satellite based calculations are difficult to estimate when compared to model based uncertainty estimation that are typically done using an ensemble of model simulations [*Bellouin et al.*, 2005]. Uncertainties in satellite based DRE estimations are from uncertainty in fluxes from CERES instrument due to calibration (±0.4 Wm^{-2}), unfiltering of TOA radiances (±0.4 Wm^{-2}), radiance to flux conversion (ADMs) over land (±0.4 Wm^{-2}), cloud contamination and uncertainty in estimating clear sky fluxes in this study. To estimate uncertainty due to cloud contamination in data analyzed, we relax the percent cloud cover from 0.01% to 1%, 5% and 10% and find the TOA DRE to vary by ±0.5 Wm^{-2}. Since F_{clr} is estimated from regression relationship between TOA shortwave flux and AOT, any uncertainty in fluxes and AOT will translate to an uncertainty in F_{clr}. Therefore, the quality of the fit of the linear regression line between shortwave flux and AOT is vital to the overall accuracy of F_{clr}. For this research, the overall correlation is about 0.7, indicating a reasonably good fit does exist. The uncertainty due to AOT is calculated from the global land aerosol forcing efficiency. Following definitions from *Zhang et al.* [2005] and *Yu et al.* [2006], the global land aerosol forcing efficiency of -28 $Wm^{-2}\tau^{-1}$ is estimated from the ratio of global mean land radiative forcing and MISR AOT ($-5.1/0.18$). Therefore, multiplying the maximum uncertainty in AOT of 0.05 [*Kahn et al.*, 2005] with efficiency of -28 $Wm^{-2}\tau^{-1}$ yields uncertainty in flux of 1.4 Wm^{-2} (or ±0.7 Wm^{-2}) [*Zhang et al.*, 2005]. Assuming that all the uncertainties are uncorrelated the total uncertainty in our DRE estimation is $(0.4^2 + 0.4^2 + 0.4^2 + 0.7^2 + 0.5^2)^{1/2}$ =

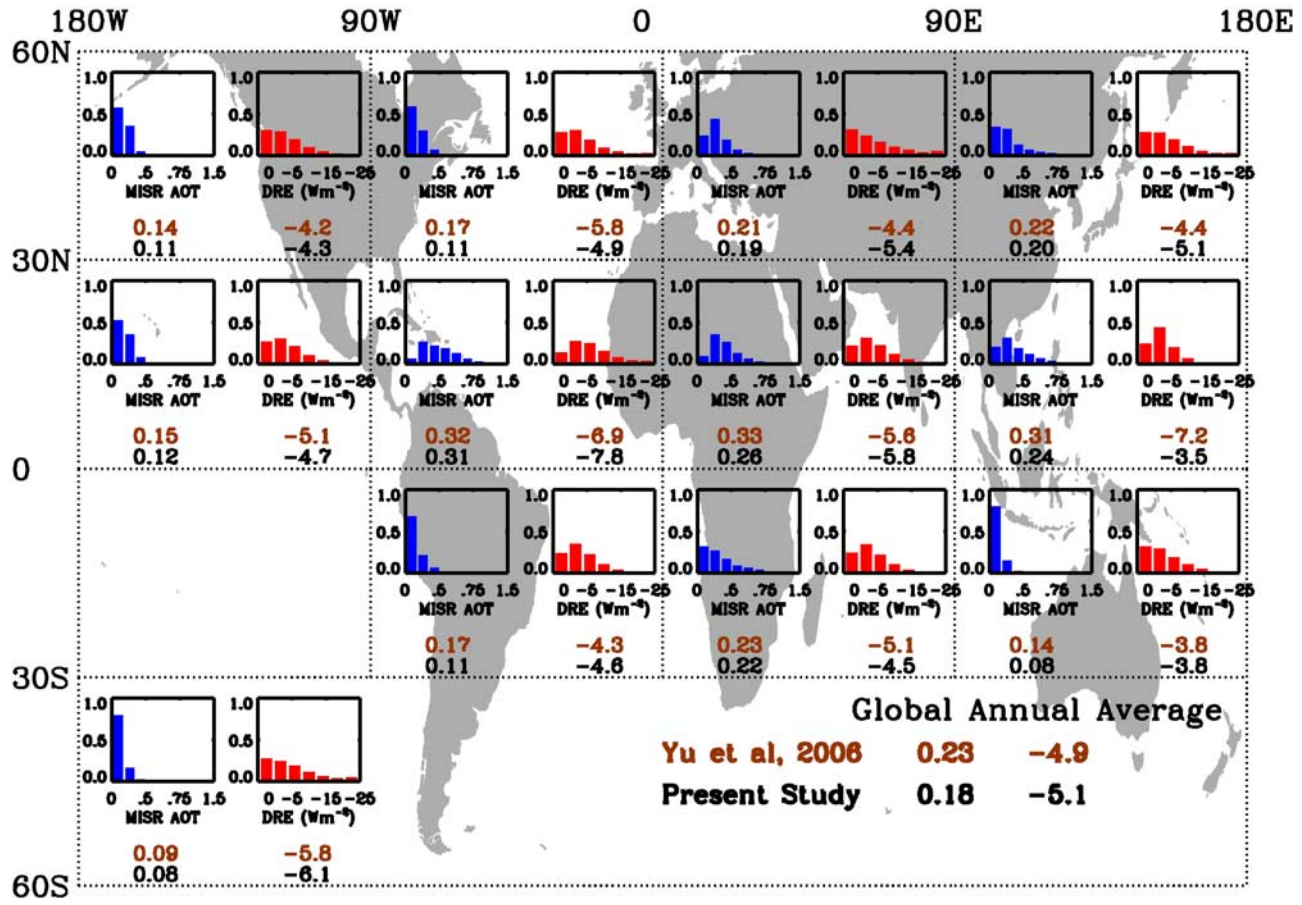

Figure 2. Regional probability density functions of MISR AOT ($\lambda = 0.558\mu$m) and TOA DRE (Wm^{-2}) over land. Also shown are mean MISR AOT and TOA DRE values for each region from the current study as well as from *Yu et al.* (2006).

1.1 Wm^{-2}. Additional uncertainties within the ADMs, due to the lack of an aerosol model, are not taken into account, due to the lack of available data to quantify them. Future improvement in retrieval algorithms, instrument calibrations and multi-angle imaging capabilities will help reduce these uncertainties.

4. Summary

[14] We have used one year of coincident MODIS, MISR and CERES data to estimate TOA shortwave direct aerosol effects over global land areas. This is entirely an observational-based estimate without using radiative transfer calculations or modeling simulations to obtain DRE. Earlier studies derived DRE over near homogeneous ocean surface using satellite data [e.g., *Christopher and Zhang*, 2004] or over land using models [*Bellouin et al.*, 2005]. Derivation of DRE over land has always been challenging due to complex and heterogeneous nature of both surface and aerosol types. Multi-angle measurements from MISR are proving to be a reliable source for aerosol information, especially over land. Furthermore, the new generation of cloud-free angular models from CERES over land provide confidence in our ability to study DRE over land. The estimated global mean clear sky DRE over land is -5.1 ± 1.1 Wm^{-2} with mean MISR AOT value within the CERES footprint of 0.18. While this is a first estimate of DRE over land from satellite measurements alone, there are several issues that need to be addressed in future studies including cloud screening, developing angular models for aerosols over land, and assessing DRE with respect to vertical distribution of aerosols.

[15] **Acknowledgments.** This research is supported by NASA's radiation sciences, an EOS grant, interdisciplinary sciences, and ACMAP programs. Pawan Gupta was supported by NASA's Earth System Science Fellowship program. The CERES SSF data that contains the merged MODIS and CERES was obtained through the NASA Langley Distributed Active Archive Systems. We thank Norman Loeb for his help with our queries.

References

Abdou, W. A., D. J. Diner, J. V. Martonchik, C. J. Bruegge, R. A. Kahn, B. J. Gaitley, K. A. Crean, L. A. Remer, and B. Holben (2005), Comparison of coincident Multiangle Imaging Spectroradiometer and Moderate Resolution Imaging Spectroradiometer aerosol optical depths over land and ocean scenes containing Aerosol Robotic Network sites, *J. Geophys. Res.*, *110*, D10S07, doi:10.1029/2004JD004693.

Anderson, T. L., et al. (2005), A-Train strategy for quantifying direct climate forcing by anthropogenic aerosols, *Bull. Am. Meteorol. Soc.*, *86*, 1795–1809.

Bellouin, N., O. Boucher, J. Haywood, and M. S. Reddy (2005), Global estimate of aerosol direct radiative forcing from satellite measurements, *Nature*, *438*, 1138–1141, doi:10.1038/nature04348.

Christopher, S. A., and J. Zhang (2004), Cloud-free shortwave aerosol radiative effect over oceans: Strategies for identifying anthropogenic forcing from Terra satellite measurements, *Geophys. Res. Lett.*, *31*, L18101, doi:10.1029/2004GL020510.

Diner, D. J., et al. (1998), Multi-angle Imaging SpectroRadiometer (MISR) description and experiment overview, *IEEE Trans. Geosci. Remote Sens.*, *36*(4), 1072–1087.

Gupta, P., F. Patadia, and S. A. Christopher (2008), Multi-sensor data product fusion for aerosol research, *IEEE Trans. Geosci. Remote Sens*, in press.

Hsu, N. C., J. R. Herman, and C. Weaver (2000), Determination of radiative forcing of Saharan dust using combined TOMS and ERBE data, *J. Geophys. Res.*, *105*(D16), 20,649–20,662.

Kahn, R. A., B. J. Gaitley, J. V. Martonchik, D. J. Diner, K. A. Crean, and B. Holben (2005), Multiangle Imaging Spectroradiometer (MISR) global aerosol optical depth validation based on 2 years of coincident Aerosol Robotic Network (AERONET) observations, *J. Geophys. Res.*, *110*, D10S04, doi:10.1029/2004JD004706.

Kaufman, Y. J., D. Tanré, and O. Boucher (2002), A satellite view of aerosols in the climate system, *Nature*, *419*, 215–223.

Kaufman, Y. J., O. Boucher, D. Tanré, M. Chin, L. A. Remer, and T. Takemura (2005), Aerosol anthropogenic component estimated from satellite data, *Geophys. Res. Lett.*, *32*, L17804, doi:10.1029/2005GL023125.

Loeb, N. G., and N. Manalo-Smith (2005), Top-of-atmosphere direct radiative effect of aerosols over global oceans from merged CERES and MODIS observations, *J. Clim.*, *18*, 3506–3526.

Loeb, N. G., S. Kato, K. Loukachine, and N. Manalo-Smith (2005), Angular distribution models for top-of-atmosphere radiative flux estimation from the clouds and the Earth's radiant energy system instrument on the Terra satellite, Part I: Methodology, *J. Atmos. Oceanic Technol.*, *22*, 338–351.

Loeb, N. G., S. Kato, K. Loukachine, and D. R. Doelling (2007), Angular distribution models for top-of-atmosphere radiative flux estimation from the clouds and the Earth's radiant energy system instrument on the Terra satellite, Part II: Validation, *J. Atmos. Oceanic Technol.*, *24*, 564–584.

Martonchik, J. V., D. J. Diner, R. A. Kahn, T. P. Ackerman, M. M. Verstraete, P. Bernard, and H. R. Gordon (1998), Techniques for the retrieval of aerosol properties over land and ocean using multiangle imaging, *IEEE Trans. Geosci. Remote Sens.*, *36*, 1212–1227.

Martonchik, J. V., D. J. Diner, K. A. Crean, and M. A. Bull (2002), Regional aerosol retrieval results from MISR, *IEEE Trans. Geosci. Remote Sens.*, *40*, 1520–1531.

Remer, L. A., and Y. J. Kaufman (2005), Aerosol effect on the distribution of solar radiation over the clear-sky global oceans derived from four years of MODIS retrievals, *Atmos. Chem. Phys. Discuss.*, *5*, 5007–5038.

Remer, L. A., et al. (2005), The MODIS aerosol algorithm, products and validation, *J. Atmos. Sci.*, *62*, 947–973.

Yu, H., et al. (2006), A review of measurement-based assessment of aerosol direct radiative effect and forcing, *Atmos. Chem. Phys.*, *6*, 613–666.

Zhang, J., S. A. Christopher, L. A. Remer, and Y. J. Kaufman (2005), Shortwave aerosol radiative forcing over cloud-free oceans from Terra: 2. Seasonal and global distributions, *J. Geophys. Res.*, *110*, D10S24, doi:10.1029/2004JD005009.

S. A. Christopher, P. Gupta, and F. Patadia, Department of Atmospheric Sciences, University of Alabama in Huntsville, 320 Sparkman Drive, Huntsville, AL 35806, USA. (sundar@nsstc.uah.edu)